Cross Regulation in Flyback Converters: Analytic Model and Solution

Chuanwen Ji, K. Mark Smith, Jr., *Member, IEEE*, Keyue M. Smedley, *Senior Member, IEEE*, and Ken King, *Member, IEEE*

***Abstract*—An analytical model for studying cross regulation among the multiple outputs of flyback converters is presented in this paper. Both the theoretical and experimental results show that the cross regulation can be improved by lowering the clamp voltage, which has not been previously reported. Many other factors, such as the leakage inductance in primary and secondary windings, the magnetizing inductance, and the air gap can also affect the cross regulation. Detailed analysis and test results are provided. Based on this model, a cost-effective passive energy regenerative clamp is proposed that allows the clamp voltage to be much lower than that of traditional RC clamps, thus improving the cross regulation and energy efficiency.**

***Index Terms*—AC–DC converter, cross regulation efficiency, DC–AC converter, flyback.**

I. Introduction

AMONG the variety of switching-mode power converters, the flyback converter is one of favorite choices among design engineers for low power applications due to its low component count, cost-effective structure, as well as its large dynamic range. However, flyback converters generally suffer from low efficiency and poor cross regulation due to its leakage inductance. In reality, no matter how the winding structure is arranged inside a transformer, the leakage inductance cannot be completely eliminated.

As switching frequency reaches megahertz level, the impact of the leakage inductance on the cross regulation becomes even more serious. In industrial practice, a weighted voltage control loop is often used to reduce a particular output error by adjusting the weighting factor. But it does not reduce the total output error, instead, it only shifts the error to the other outputs [1]. Some previously published papers [2]–[5] have revealed the relations between the leakage inductance and cross regulation to some extent. However, quantitative relationship describing the effects of the leakage inductance among windings on the cross regulation has not been reported so far. Paper [6] has shown certain insight into this issue; however, it converts the leakage inductance in primary winding to the secondary side, which makes the predicted results difficult to be matched by experiments. An extensive analysis based on coupled inductor is given in [7] for multiple output flyback converters, which shows the frequency dependant nature of multiple output converters. A model of cross regulation was given in [8] for converters containing coupled inductors.

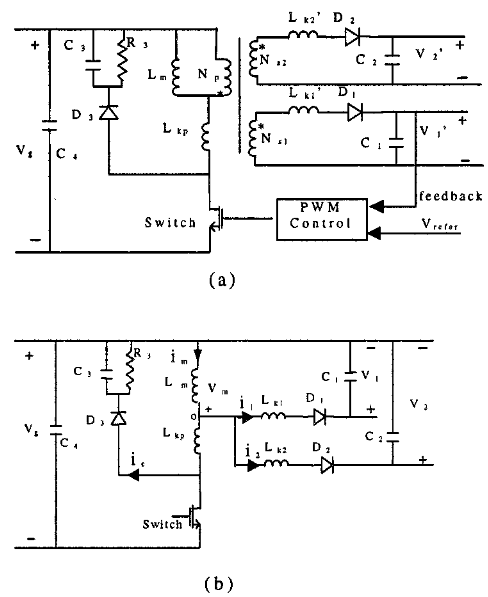

Fig. 1. (a) Typical flyback converter of two outputs. (b) Equivalent transformer model on the primary side for analyzing the cross regulation.

This paper presents an analytical model to explore the cross regulation mechanism inside a flyback converter and to investigate the crucial factors that affect cross regulation in a multiple-output flyback converter. Based on this model, a cost-effective solution to improve the cross regulation and efficiency is provided. The analytical model of cross regulation is derived in Section II, the analytical predictions and experimental results are presented in Sections III and IV, a solution to improve the cross regulation is proposed in Section V, and a conclusion is provided in Section VI.

II. Analytical Model of Cross Regulation in Flyback Converter

A flyback converter cyclically stores energy in its transformer from the input dc source when its switch is on and then releases this stored energy into its outputs after the switch is turned off. By adjusting the amount of energy stored and released per-cycle, the output voltage can be regulated. Fig. 1(a) shows a typical two-output flyback converter topology with an RC clamp (C_3, R_3, and D_3) dissipating the energy from the leakage inductance, L_{kp}, each cycle when the switch is turned off and limiting the voltage stress on the switch. In Fig. 1(a), the transformer is

Manuscript received January 20, 1999; revised November 28, 2000. Recommended by Associate Editor P. K. Jain. This work was supported by Cherokee International, LLC and the University of California MICRO program.

C. Ji, K. M. Smith, Jr., and K. M. Smedley are with the Department of Electrical and Computer Engineering, University of California, Irvine, CA 92697 USA (e-mail: Smedley@uci.edu).

K. King is with the Cherokee International, LLC, Tustin, CA 92680 USA.

Publisher Item Identifier S 0885-8993(01)02197-4.

0885–8993/01$10.00 © 2001 IEEE

modeled as an ideal transformer with a magnetizing inductance, L_m, and equivalent leakage inductance, L_{kp}, L_{k1} and L_{k2}, corresponding to those of primary winding, secondary winding 1, and winding 2, respectively. Compared with the leakage inductance, the resistance of windings is small enough to be neglected for simplicity of the analysis.

By converting the secondary sides to the primary side of the transformer, an equivalent circuit is derived as shown in Fig. 1(b). It is a consequential platform for quantitative analysis of the cross regulation in the flyback converter.

Assuming that the load in output 2 of the converter shown in Fig. 1 is lighter than that in output 1, the current waveforms in both outputs can be plotted for one switching cycle as shown in Fig. 2 when operating in discontinuous current mode (DCM). In Fig. 2, I_c is the current flowing to the RC clamp and I_m is the equivalent magnetizing current.

When the switch is turned on at t_0, the magnetizing current will increase with a slope of $V_g/(L_m + L_{kp})$

$$i_m(t) = \frac{V_g}{L_m + L_{kp}} \cdot t \tag{1}$$

where V_g is converter input dc voltage.

At the moment t_1 when the switch is turned off, a large portion of the magnetizing current will flow into the capacitor C_3 of RC clamp due to the leakage inductance in the output loops. The corresponding equivalent circuit during T_1 is shown in Fig. 3(a) where the capacitance of $C_1, C2$ and C_3 are assumed to be large enough so that the voltages across them could be considered as constant during the entire switching cycle. In order to simplify the analysis, the voltage drops in all diodes are neglected.

The sum of currents at node O equal zero

$$i_m = i_c + i_1 + i_2. \tag{2}$$

Differentiating of (2) yields

$$\frac{di_m}{dt} = \frac{di_c}{dt} + \frac{di_1}{dt} + \frac{di_2}{dt}. \tag{3}$$

Substitution of the current changing rates of i_m, i_c, i_1 and i_2 into (3) gives

$$-\frac{V_{m1}}{L_m} = \frac{V_{m1} - V_c}{L_{KP}} + \frac{V_{m1} - V_1}{L_{K1}} + \frac{V_{m1} - V_2}{L_{K2}}. \tag{4}$$

Let $K_1 = L_m/L_{k1}$, $K_2 = L_m/L_{k2}$, and $K_p = L_m/L_{kp}$, solving (4) for V_{m1} yields

$$V_{m1} = \frac{K_1 V_1 + K_2 V_2 + K_p V_c}{1 + K_1 + K_2 + K_p}. \tag{5}$$

During T_1 interval, the current flowing into C_3 is

$$i_c(t) = \frac{(V_{m1} - V_c)}{L_{kp}} \cdot t + I_0 \tag{6}$$

where I_0 is the magnetizing current at the moment when the switch is turned off.

The diode D_3 conduction time, T_1, is obtained by letting $i_c(t) = 0$

$$T_1 = \frac{L_m I_0}{K_p} \cdot \frac{1 + K_1 + K_2 + K_p}{V_c + V_c K_1 + V_c K_2 - K_1 V_1 - K_2 V_2}. \tag{7}$$

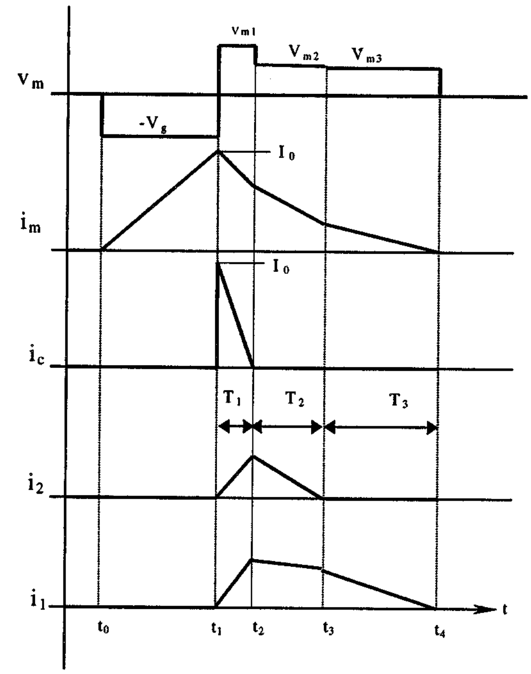

Fig. 2. Ideal voltage and current waveforms during one switching cycle. V_m: magnetizing voltage; i_m: magnetizing current; i_c: current into the capacitor of RC clamp; i_1 and i_2: currents through the output windings.

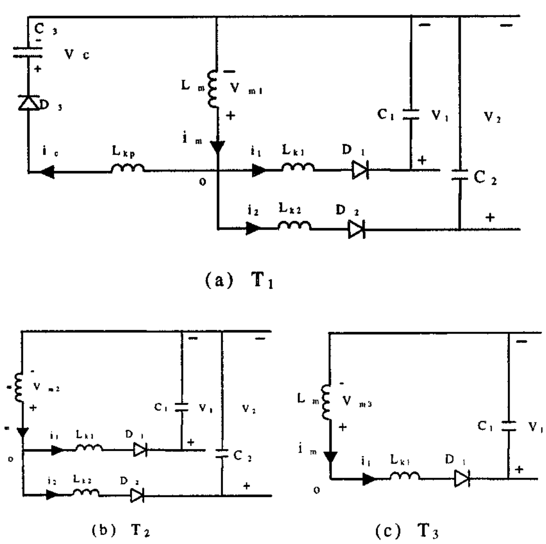

Fig. 3. Equivalent circuits during T_1, T_2 and T_3.

The currents of output 2 and output 1 during T_1 are

$$i_2(t) = \frac{(V_{m1} - V_2)K_2}{L_m} \cdot t \tag{8}$$

$$i_1(t) = \frac{(V_{m1} - V_1)K_1}{L_m} \cdot t. \tag{9}$$

At t_2, the end of T_1, when the current in capacitor C_3 drops to zero, the peak current in output 2 is obtained by substitution of (7) into (8)

$$I_{2PK2} = \frac{K_2 I_0 (1 + K_1 + K_2 + K_p)(V_{m1} - V_2)}{K_p(V_c + V_c K_1 + V_c K_2 - K_1 V_1 - K_2 V_2)}. \tag{10}$$

In similar way, the instantaneous current of output 1 at t_2 can be derived

$$I_{1PK2} = \frac{K_1 I_0 (1 + K_1 + K_2 + K_p)(V_{m1} - V_1)}{K_p (V_c + V_c K_1 + V_c K_2 - K_1 V_1 - K_2 V_2)}. \quad (11)$$

After the current $i_c(t)$ through capacitor C_3 drops to zero, the diode D_3 is reverse biased. The equivalent circuit during T_2 is reduced as shown in Fig. 3(b)

$$i_m = i_1 + i_2. \quad (12)$$

Differentiating above (12) yields

$$\frac{di_m}{dt} = \frac{di_1}{dt} + \frac{di_2}{dt}. \quad (13)$$

Substitution of the current changing rates of i_m, i_1 and i_2 into (13) gives

$$-\frac{V_{m2}}{L_m} = \frac{V_{m2} - V_2}{L_{k2}} + \frac{V_{m2} - V_1}{L_{K1}} \quad (14)$$

i.e.,

$$V_{m2} = \frac{K_1 V_1 + K_2 V_2}{1 + K_1 + K_2}. \quad (15)$$

The current in output 2 during T_2 is

$$i_2(t) = \frac{V_{m2} - V_2}{L_{k2}} \cdot t + I_{2PK2}. \quad (16)$$

The current $i_2(t)$ will drop to zero before $i_1(t)$ does due to its lighter load and higher voltage at the output, so that T_2 can be obtained by letting $i_2(t) = 0$, as seen in (17), shown at the bottom of the page.

The current of output 1 during T_2 is

$$i_1(t) = \frac{V_{m2} - V_1}{L_{k1}} \cdot t + I_{1PK2} \quad (18)$$

The instantaneous current in output 1 at time t_3 when the current in output 2 drops to zero can be obtained by substitution of (17) into (18)

$$I_{1PK3} = \frac{K_1 I_0 (V_2 - V_1)}{V_2 + V_2 K_1 - V_1 K_1} \quad (19)$$

Equation (19) states that if the two output voltages are equal, $I_{1pk3} = 0$, which means that the two output currents will drop to zero simultaneously and have similar triangle waveform as shown in Fig. 4(a).

After t_3, only L_m and L_{k1} have current, the equivalent circuit during T_3 is shown in Fig. 3(c)

$$i_1(t) = -\frac{V_1}{L_{k1} + L_m} \cdot t + I_{1PK3}. \quad (20)$$

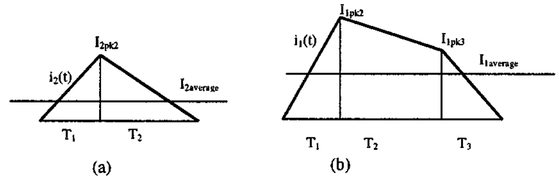

Fig. 4. Ideal current wave forms in the secondary windings.

T_3 is obtained by letting $i_1(t) = 0$

$$T_3 = \frac{I_0 L_m (V_2 - V_1)(1 + K_1)}{V_1 (V_2 + V_2 K_1 - V_1 K_1)}. \quad (21)$$

From the above analysis, the current in output 2 and output 1, after the switch is turned off, are calculated and shown in Fig. 4(a) and (b), respectively.

The average current of output 2 during one switching cycle is (22), shown at the bottom of the next page, and the average current of output 1 is (23), shown at the bottom of the next page, where

$$\begin{aligned} M = {} & K_p K_2 V_2^2 + K_p K_1 V_1 V_2 - K_p K_1 V_c V_2 + K_1 V_1 V_2 \\ & - K_p V_c V_2 - K_p K_2 V_2 V_c - K_p K_2 V_1 V_2 + K_p V_1 V_2 \\ & + V_1 V_2 + K_p K_1 V_c V_1 - K_p K_1 V_1^2 - K_1 V_1^2 \\ & + K_p K_2 V_c V_1 \end{aligned}$$

The ratio of the two output average currents is obtained by dividing (22) by (23)

$$\frac{I_{2\,\text{average}}}{I_{1\,\text{average}}} = \frac{K_2 V_1 (V_2 + V_2 K_1 + V_2 K_p - K_1 V_1 - K_p V_c)}{K_1 M}. \quad (24)$$

Equation (24) is the base to derive the output error expressions. In this paper, two typical cases will be discussed.

In case 1, it is assumed that only one output, say output 1, has feedback control to keep its output constant no matter how its load varies, and the uncontrolled output 2, whose voltage is cross regulated through the output 1, has no external load except a pre-load resistor R_2. In actual design practice, the pre-load resistor is used to prevent an momentary high over voltage at the output from occurring under no-load conditions. Its resistance has been converted to primary side in (26). In this case, the worst cross regulation occurs at the output2 when it has light load and the output 1 is in a heavy load condition. The voltage of output 2 is assumed to deviate from output 1 by an error ΔV_2

$$V_2 = V_1 + \Delta V_2 \quad (25)$$

$$I_{2\,\text{average}} = \frac{V_2}{R_2}. \quad (26)$$

Substitution of (25) and (26) into (24) gives an expression for the average current I_1 average presented in the Appendix (A1). It shows that the error of output 2, ΔV_2, is a function

$$T_2 = \frac{L_m I_0}{K_p} \cdot \frac{(1 + K_1 + K_2)(K_1 V_1 + K_p V_c - V_2 - V_2 K_1 - V_2 K_p)}{(V_c + V_c K_1 + V_c K_2 - K_1 V_1 - K_2 V_2)(V_2 + V_2 K_1 - K_1 V_1)} \quad (17)$$

with such variables as V_c (the clamp voltage of capacitor), K_1 (winding 1 leakage inductance factor, L_m/L_{k1}), K_2 (winding 2 leakage inductance factor, L_m/L_{k2}), and R_2 (pre-load resistance at output 2) as well as the load current in the regulated output.

In case 2, the weighted output control is used. A typical flyback converter with weighted voltage control is shown in Fig. 5.

In the steady state, the algorithmic mechanism of the weighted voltage control can be expressed as

$$k_1 \cdot V_1 + k_2 \cdot V_2 = V_{\mathrm{ref}\,w} \tag{27}$$

where k_1 and k_2 are constant and $V_{\mathrm{ref}\,w}$ is the reference voltage of compensator.

Differentiating (27) yields

$$k_1 \cdot \Delta V_1 + k_2 \cdot \Delta V_2 = 0. \tag{28}$$

Define the weighting factors of the two outputs as $K_{w1} = k_1/(k_1+k_2)$ and $K_{w2} = k_2/(k_1+k_2)$ respectively, thus $K_{w1} + K_{w2} = 1$ and (28) becomes

$$K_{w1} \cdot \Delta V_1 + K_{w2} \cdot \Delta V_2 = 0 \tag{29}$$

where $0 < K_{w1}, K_{w2} < 1$.

Since all reflected output voltages are identical in an ideal multiple output transformer, output errors, ΔV_1 and ΔV_2, can be viewed as their deviation from the reflected output voltage, namely, $\Delta V_1 = V_1 - V_{\mathrm{refl}}$ and $\Delta V_2 = V_2 - V_{\mathrm{refl}}$, therefore

$$V_1 = \frac{-K_{w2}}{1-K_{w2}} \cdot \Delta V_2 + V_{\mathrm{refl}} \tag{30}$$

$$V_2 = \Delta V_2 + V_{\mathrm{refl}}. \tag{31}$$

Substitution of (30) and (31) to the basic (24) yields an expression for I_2 average/I_1 average as shown in (A2), which provides a closed-form equation for analyzing cross regulation in flyback converters with weighted output control.

The analysis of cross regulation from the closed-form expressions derived is readily done with standard computational software. In the next two sections, the analytical model will be verified by experiments and the analytic results will be presented as well.

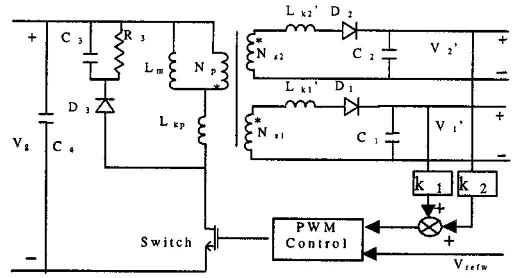

Fig. 5. Typical flyback converter with weighted voltage control.

III. Relation Between the Clamp Voltage and the Output Voltage Cross Regulation

A. *Case 1. One Output Is Regulated While the Other Is Open (Cross Regulated)*

1) Error of the Unregulated Output versus the Load Variation of the Regulated Output: A flyback converter used in experiments has two outputs, V_1 and V_2. Output1 is directly fed back to regulate its output voltage while output2 is cross regulated through output1. The experimental flyback converter has 24 Ω and 66.7 Ω resistors at the output 1 and output 2, respectively, as commonly used pre-loads to avoid inapropriate over voltage on its outputs when without external loads. Its transformer parameters are listed in Table I and dc input voltage is 170 V. All boxed curves in the figures shown in this paper are experimental results and no boxed curves are from modeling prediction.

In the flyback converter design procedure, the clamp voltage is selected to meet the voltage stress requirement of the switch. Up to now, there is no literature reporting the fact that the clamp voltage affects the cross regulation on the multiple outputs. The study in this work has revealed a strong correlation between the clamp voltage and the cross regulation. Both the analytical prediction and experimental results, as shown in Fig. 6, indicate that, during heavy load in the regulated output, the output error in the unregulated output is reduced by 44 percent when decreasing the clamp voltage V_c from 160 V to 100 V under the listed circuit condition. Furthermore, it is found that if the clamp voltage is designed slightly greater than, but not equal to,

$$\begin{aligned} I_{2\,\mathrm{average}} &= \frac{1}{T} \cdot \left[\frac{1}{2} \cdot I_{2PK2} \cdot (T_1 + T_2) \right] \\ &= \frac{K_2 L_m I_0^2}{2 \cdot K_p T} \cdot \frac{(-K_1 V_1 - K_p V_c + V_2 + V_2 K_1 + V_2 K_p)}{[(V_2 + K_1 V_2 - K_1 V_1)(K_2 V_2 + K_1 V_1 - V_c - K_1 V_c - K_2 V_C)]} \end{aligned} \tag{22}$$

$$\begin{aligned} I_{1\,\mathrm{average}} &= \frac{1}{T} \cdot \left[\frac{1}{2} \cdot T_1 \cdot I_{1PK2} + \frac{1}{2}(I_{1PK2} + I_{1PK3}) \cdot T_2 + \frac{1}{2} I_{1PK3} \cdot T_3 \right] \\ &= \frac{K_1 L_m I_0^2}{2 K_p T} \cdot \frac{M}{V_1(V_2 + K_1 V_2 - K_1 V_1)(K_2 V_2 + K_1 V_1 - V_c - K_1 V_c - K_2 V_c)} \end{aligned} \tag{23}$$

TABLE I
FLYBACK TRANSFORMER PARAMETERS

Turns of primary	36
Turns of output 1	3
Turns of output 2	4
L_m	293μH
L_{kp}	9.9μH
L_{k1}(converted to prim. side)	9.8μH
L_{k2}(converted to prim. side)	9.8μH
R_1 (Pre-load in output 1)	24Ω
R_2 (Pre-load in output 2)	66.7Ω
V_1 (regulated voltage of output1)	5V
V_2 (Normal voltage of output2)	6.7V
V_{ref}(output reflected voltage)	60V

the output reflected voltage, the output error in the unregulated output is minimized.

2) Error of the Unregulated Output versus the Load Variation of Its Own and the Regulated Output: The prior section notes how load variation in the regulated output affects the output error of the unregulated output when it has only a pre-load resistance. It is also important to know the output regulation versus the load variation of both outputs. The output error of the unregulated output corresponding to the variation of both loads is shown by a 3-dimentional plots in Fig. 7(a) and (b) for the clamp voltage of 160 V and 100 V, respectively. It is shown that the error is reduced dramatically by lowering the clamp voltage. Moreover, the extensive flat area in the central part of the Fig. 7(a) and (b) indicates that the better cross regulation occurs when both load currents are higher than a certain level, above which the cross regulation is not dominantly influenced by leakage inductance and other factors.

B. Case 2. Output Errors in Flyback Converter With Weighted Voltage Control

Based upon the modeling analysis, the output error can be analytically predicted and plotted as shown in Fig. 8 for a clamp voltage of 160 V and Fig. 9 for a clamp voltage of 100 V in terms of arbitrarily-chosen weighting factors, i.e., $K_{w1} = 0.8$, $K_{w2} = 0.2$. Figs. 8 and 9 indicate that weighted voltage control by no means reduces overall error but redistributes it among the outputs. It can reduce the particular output error by adjusting the weighting factor at the cost of degrading the others since it does not render a mechanism for outputs to track each other. However, lowering clamp voltage can overall reduce both output errors in the flyback converter. The analytical outcomes can foretell output error and help engineers to make appropriate tradeoff among the weighted factors, the clamp voltage, and pre-load currents to satisfy the regulation specification of each output.

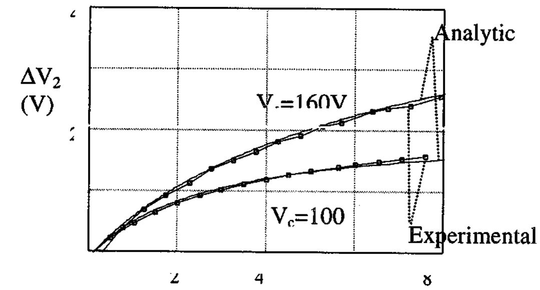

Fig. 6. Both analytic and experimental results show that the error of the unregulated output is reduced when lowering the clamp voltage.

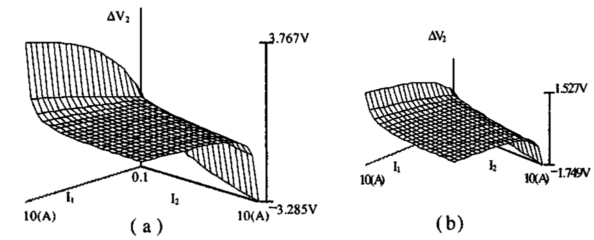

Fig. 7. Three-dimensional plots of the unregulated output error: (a) $V_c = 160$ V and (b) $V_c = 100$ V.

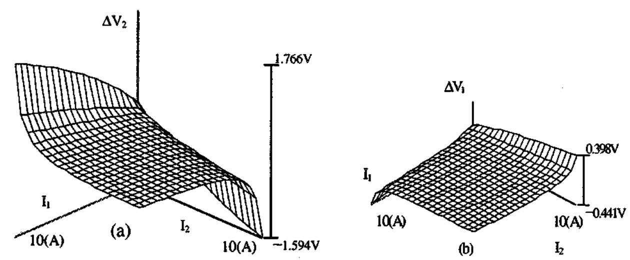

Fig. 8. Predicted output error in a flyback converter with weighted voltage control where the clamp voltage $V_c = 160$ V, $K_{w1} = 0.8$, $K_{w2} = 0.2$, $K_1 = K_2 = K_p = 30$: (a) the error at output 2 and (b) the error at output 1.

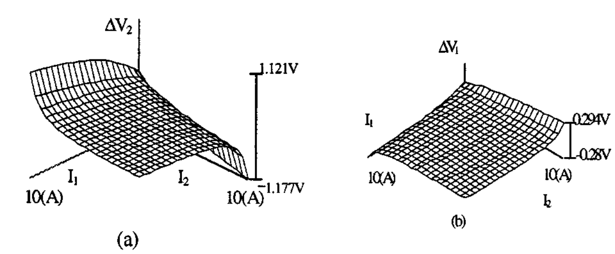

Fig. 9. Predicted output error in a flyback converter with weighted voltage control where the clamp voltage $V_c = 100$ V, $K_{w1} = 0.8$, $K_{w2} = 0.2$, $K_1 = K_2 = K_p = 30$: (a) the error at output 2 and (b) the error at output 1.

IV. EFFECT OF THE LEAKAGE INDUCTANCE ON THE OUTPUT VOLTAGE CROSS REGULATION

A commonly used method to reduce the error in the unregulated outputs is to decrease its pre-load resistance. However, this yields more loss. Analysis shows that adding a small inductor to the unregulated output reduces its output error and improves the cross regulation as shown in Fig. 10. As an example, a 0.36 uH inductor was inserted in series with the winding of the unregulated output 2. Curve a and b show the predicted and measured errors when there is no extra inductor. As shown by curve c (predicted) and d (experimental) in Fig. 10, the error is reduced by 40% when heavy load is applied to output 1 compared with the error in curve a (experimental) and b (predicted). However, its output voltage will actually drop more during very light load in the regulated output 1 because the larger inductance in output 2 causes less energy flow toward its output. One way to reduce this drop and regain its original output is to increase its pre-load resistance as shown by curve e in Fig. 10, as a consequence, the efficiency will be improved. In practice, adding a small inductor in the unregulated outputs can be realized by arrangement of winding structure in the window of transformer core to shift the leakage inductance distribution. For instance, a desired larger leakage inductance in the winding of the unregulated outputs can be achieved by placing it in the outer layer of the core window.

In Fig. 11, both modeling predictions and experimental results show that larger leakage inductance in the primary winding will result in a smaller error in the unregulated output. In the experiment, the added inductance is 20 uH.

Magnetizing inductance can be adjusted by varying the air gap between the magnetic cores, which does not change the leakage inductance much among the windings if the fringe effect is not significant. Fig. 12 shows that the cross regulation is improved, if the magnetizing inductance is increased by altering the gap while the leakage inductance is assumed to be unchanged. It means that reduction of the gpap will improve the cross regulation, although other considerations may make this inappropiate.

The well matched experimental and analytical results, as shown in Figs. 6, 10 and 11, demonstrate that the analytic model closely represents the mechanism of the cross regulation in flyback converters.

V. Solution: Energy Regenerative Clamp

Both the analytical model and experimental results shown in above section have clearly manifested that cross regulation in multiple output flyback converters can be greatly improved when the clamp voltage is maintained slightly above the reflected output voltage. However, using a traditional RC clamp to keep this voltage low results in high power losses. For instance, the loss in the RC clamp shown in Fig. 1(a) can be found by integration of the product of the clamp voltage V_c and charging current i_c during the period of switch turn off

$$\begin{aligned}\mathbf{P}_c &= f\cdot\int_0^T V_c\cdot\mathbf{i}_c(t)\cdot dt\\ &= \frac{1}{2}\cdot L_m\cdot I_0^2\\ &\quad\cdot\frac{(1+K_1+K_2+K_p)\cdot f}{\left[1+K_1\cdot\left(1-\frac{V_1}{V_c}\right)+K_2\cdot\left(1-\frac{V_2}{V_c}\right)\right]\cdot K_p}.\end{aligned}\tag{32}$$

From (32), the energy loss in the RC clamp can be plotted in terms of the clamp voltage as shown in Fig. 13, which indicates that lowering the clamp voltage leads to more losses, especially when the clamp voltage approaches the reflected output voltage

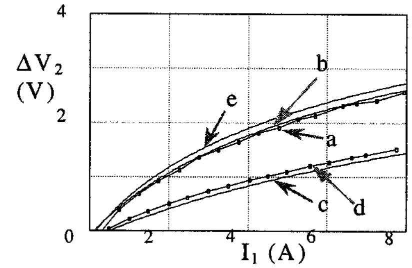

Fig. 10. Adding a small inductor in the loop of the unregulated output reduces its output error. a and b: $R_2 = 66.7\ \Omega$ and without an extra inductor, c and d: $R_2 = 66.7\ \Omega$ and $L_{\rm extra} = 0.36\ \mu$H, and e: $R_2 = 203\ \Omega$ and $L_{\rm extra} = 0.36\ \mu$H.

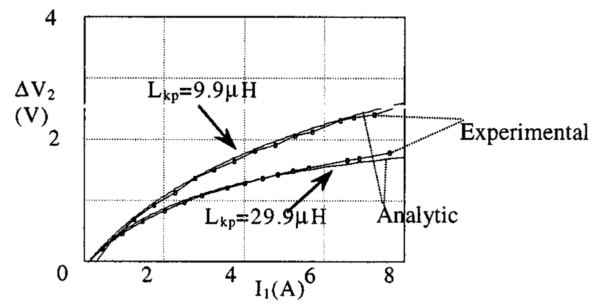

Fig. 11. Larger leakage inductor in primary side reduces the error of the unregulated output, where the initial leakage inductance is 9.9 μH and an added extra inductor is 20 μH.

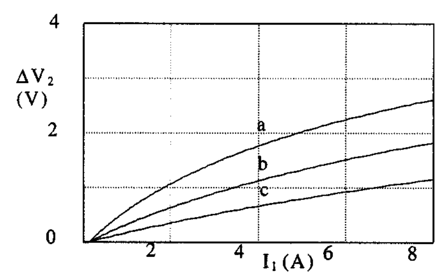

Fig. 12. Larger magnetizing inductance results better cross regulation:(a) $K_1 = K_2 = K_{LP} = 30$, (b) $K_1 = K_2 = K_{LP} = 60$, and (c) $K_1 = K_2 = K_{LP} = 120$.

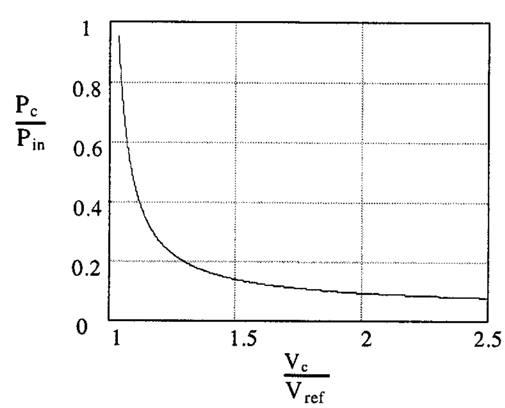

Fig. 13. Loss in RC clamp increases when the clamp voltage approaches reflected output voltage.

of V_1 and V_2. It is necessary to make a tradeoff between the cross regulation and efficiency if an RC clamp is used.

Equation (32) illustrates several important characteristics of the RC clamp circuit. For a certain resistance of R_3 in the RC clamp, the clamp voltage is determined by the energy into the capacitor. Since it is proportional to the converted overall power, $1/2 * L_m * I_0^2$, the clamp voltage varies with load currents and so does the cross regulation. However, the lost energy is independent of the input voltage. Therefore, the cross regulation of a flyback converter with an RC clamp remains the same for the universal input voltage range if the feedback control has an infinite gain. It is the simplest and cheapest approach to limit the voltage stress cross the switch, but efficiency suffers.

To overcome the defect in the RC clamp, an energy regenerative clamp to losslessly maintain a low clamp voltage is proposed as shown in Fig. 14. This clamp uses an extra winding, N_R that shares the *same core of the transformer*. A similar clamp winding for a forward converter was proposed in [9]. When the switch is turned off, the transformer's magnetizing and primary leakage inductance will initially conduct through C_3 and D_3, clamping the voltage across the switch to $V_g + V_c$. At this moment, diode D_4 is reversely biased, no current flows through the clamp winding, and the energy in the leakage inductance is temporally stored in capacitor C_3. It is assumed that the capacitance of C_3 is large enough that the voltage across it approximately maintains constant from cycle to cycle. When the switch is turned on, the magnetizing inductance of the transformer will be charged by two energy sources. Initially it will be charged by C_3 through the clamp winding N_r to transformer core until the voltage across C_3 drops to the reflected input voltage, $V_g \cdot N_r/N_p$. After that, diode D_4 is reverse biased and the transformer will be energized from the input voltage source V_g. The current waveforms are shown in Fig. 15, where I_p and I_c are the currents through the primary winding and the clamp capacitor, C_3, respectively.

When the switch is on, diode D_3 and all the diodes in the output are reverse biased, and the voltage on the capacitor C_3 is approximately equal to that of the clamp winding N_r if the voltage drops on diode D_4 and switch are neglected. During the switch-on period, the voltages of primary and clamp winding satisfy

$$V_{c3} = \frac{N_r}{N_p} \cdot V_g. \tag{33}$$

Equation (33) indicates that the clamp voltage is determined by the designed turns of the clamp winding. It must be greater than the output reflected voltage so that the energy stored in the magnetic core can be converted to the secondary side during the switch-off period, otherwise it will be totally transferred to capacitor C_3, i.e.,

$$V_{c3} > \frac{V_o \cdot N_p}{N_s}. \tag{34}$$

Substitution of (33) into (34) gives design criteria for the clamp winding

$$N_r > \frac{V_o \cdot N_p^2}{V_g \cdot N_s}. \tag{35}$$

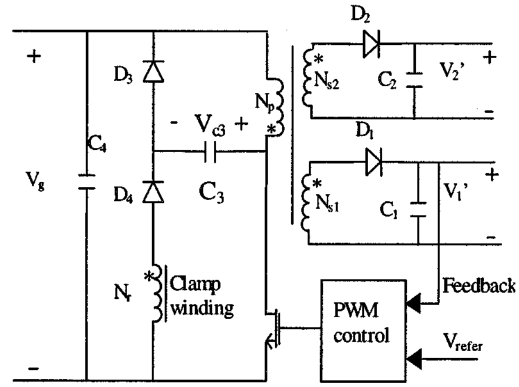

Fig. 14. Proposed energy regenerative clamp.

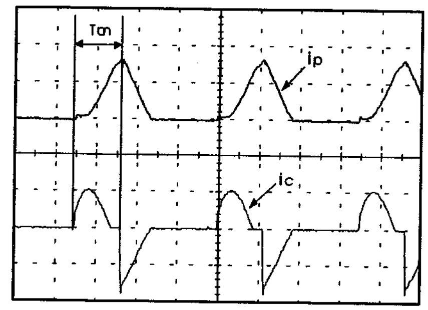

Fig. 15. Measured currents through the primary winding and the clamping capacitor C_3 in flyback converter with energy regenerative clamp.

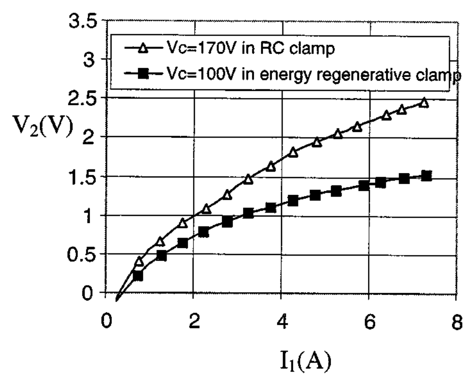

Fig. 16. Comparison of the errors in the unregulated output2 of the flyback converter with the energy regenerative clamp and that with RC clamp.

Voltage stress across switch is

$$V_{\mathrm{sw}} = V_g + V_c = V_g \cdot \left(1 + \frac{N_r}{N_p}\right). \tag{36}$$

Equation (36) shows that the voltage stress across the switch is controllably determined by the turns of the clamp winding and does not change with the variations of leakage inductance nor the load currents unlike that in the RC clamp. But, the clamp voltage is proportional to the input rms voltage, therefore, the cross regulation at high end (i.e., 230 V ac) will be worse than that at low end (i.e., 115 V ac) for an universal input.

Comparative experiments were conducted in a flyback converter with identical parameters listed in Table I. When the flyback converter used the RC clamp, the clamp voltage was designed as 170 V at full load (+5 V output1 is 8 A). Under this condition, the output error in the $+6.7$ V output2 is more than 2.6 V as shown in Fig. 16. Using the same flyback converter, a new clamp winding of 21 turns was added to the transformer. This winding gives a clamp voltage of 100 V when the input voltage is about 120 V ac. After the proposed energy regenerative clamp was employed, the error on $+6.7$ V output was only 1.5 V with the same full load current on $+5$ V output as shown by the curve with diamond in Fig. 16. It was reduced by 42% compared with that of the RC clamp. However, because of the dependency of the clamp voltage on the input voltage, when the input voltage was increased to be 220 V ac, the clamp voltage becomes 170 V, and cross regulation is close to that of the RC clamp. Another advantage of this energy regenerative clamp is that it improves overall efficiency by regenerating the energy stored in the primary leakage inductance, rather than dissipating in the resistor of the RC clamp. In the experimental flyback converter after the clamp is applied, its efficiency is improved by 7.7% at full load condition.

VI. Conclusion

The model for analyzing cross regulation among the outputs of flyback converter is presented and verified by experiments. The cross regulation of a multioutput flyback converter can be significantly improved by lowering the clamp voltage, especially to slightly above the reflected output voltage. However, use of a traditional RC clamp causes more loss.

1) Larger leakage inductance in the secondary windings leads to better cross regulation of that output when it is lightly loaded.
2) Larger leakage inductance in the primary side can be beneficial to improve the cross regulation of multiple output flyback converters. However, it results more loss in a traditional RC clamp.
3) Reducing core gap to achieve larger magnetizing inductance in the flyback converter design will improve cross regulation, when this can be accomodated.

The traditional RC clamp is the simplest and cheapest approach to limit the voltage stress across the switch. Its clamp voltage is dependent on the output load of converters but not on the input voltage, which leads to the same cross regulation for universal input applications. However, since it is a dissipative clamp, decreasing its designed clamp voltage to achieve better cross regulation is at the cost of efficiency. Therefore, in the design procedure, it is indispensable to make a tradeoff between the cross regulation and efficiency when an RC clamp is used. The proposed energy regenerative clamp allows the clamp voltage to be much lower than that of RC clamp without yielding losses by recovering leakage energy, consequently overcoming the defect in the RC clamp. Its clamp voltage doesn't alter as a of the load's variation unlike with the RC clamp. It does not require an extra magnetic core, since the clamp winding shares the same core with the transformer. The proposed clamp uses the same number of components as the RC clamp, therefore, it is a cost-effective approach to improve both cross regulation and efficiency in multiple output flyback converters. However, due to the dependency of its clamp voltage on the input voltage, the cross regulation cannot be maintained the same for universal input applications. It will suffer at the high end, i.e., 230 V ac, when the clamp is designed for low end input, i.e., 115 V ac.

Appendix

A closed-form equation for analyzing the cross regulation of flyback converters with single voltage feedback control in term of $v2$ can be determined from the derived expression for the average current I_1 average

$$I_1 average = \frac{K_1 S}{K_2 V_1 R_2(-K_p V_c + V_1 + K_1 \Delta V_2 + K_p V_1 + K_p \Delta V_2 + \Delta V_2)}$$

where

$$\begin{aligned} S = {} & K_p K_2 V_1^2 \Delta V_2 + 2K_p K_2 V_1 \Delta V_2^2 \\ & + K_p K_1 V_1^2 \Delta V_2 - K_p K_1 V_1 V_c \Delta V_2 + K_1 V_1^2 \Delta V_2 \\ & - K_p V_1^2 V_c - 2K_p V_1 V_c \Delta V_2 \\ & - K_p K_2 V_1 V_c \Delta V_2 + K_p V_1^3 + 2K_p V_1^2 \Delta V_2 \\ & + V_1^3 + 2V_1^2 \Delta V_2 \\ & + K_p K_2 \Delta V_2^3 + K_p K_1 V_1 \Delta V_2^2 - K_p K_1 V_c \Delta V_2^2 \\ & + K_1 V_1 \Delta V_2^2 \\ & - K_p V_c \Delta V_2^2 - K_p K_2 V_c \Delta V_2^2 + K_p V_1 \Delta V_2^2 + V_1 \Delta V_2^2. \end{aligned} \tag{A1}$$

A close-form equation for analyzing the cross regulation of flyback converters with weighted voltage control in term of $v2$ can be determined from the derived expression for the ratio of average current I_2 average to I_1 average

$$\frac{I_2 average}{I_1 average} = \frac{K_2}{K_1} \cdot (K_{w1} V_{\text{refl}} - K_{w2} \Delta V_2) \cdot \frac{X}{Y} \tag{A2}$$

where

$$\begin{aligned} X = {} & K_{w2} K_p V_c - K_p V_c + \Delta V_2 \\ & - K_{w2} \Delta V_2 + V_{\text{refl}} - K_{w2} V_{\text{refl}} \\ & + K_1 \Delta V_2 + K_p \Delta V_2 - K_p K_{w2} \Delta V_2 \\ & + K_p V_{\text{refl}} - K_p K_{w2} V_{\text{refl}} \end{aligned}$$

and

$$\begin{aligned} Y = {} & K_p K_2 \Delta V_2^2 - 3K_{w2} \Delta V_2 V_{\text{refl}} \\ & + 2K_{w2}^2 \Delta V_2 V_{\text{refl}} + K_1 \Delta V_2 V_{\text{refl}} \\ & - K_1 K_{w2} \Delta V_2^2 + \Delta V_2 V_{\text{refl}} + V_{\text{refl}}^2 \\ & - K_{w2} \Delta V_2^2 + K_{w2}^2 \Delta V_2^2 - 2K_{w2} V_{\text{refl}}^2 \\ & + K_{w2}^2 V_{\text{refl}}^2 - 3K_p K_{w2} \Delta V_2 V_{\text{refl}} \\ & + 2K_p K_{w2}^2 \Delta V_2 V_{\text{refl}} - K_p K_{w2} \Delta V_2^2 \\ & + K_p K_{w2}^2 \Delta V_2^2 + K_p \Delta V_2 V_{\text{refl}} \\ & - 2K_p K_{w2} V_{\text{refl}}^2 + K_p K_{w2}^2 V_{\text{refl}}^2 \\ & + K_p K_1 K_{w2} V_c \Delta V_2 + K_p V_{\text{refl}}^2 \\ & + K_p K_1 \Delta V_2 V_{\text{refl}} - K_p K_1 K_{w2} \Delta V_2^2 \\ & - K_p K_1 K_{w2} \Delta V_2 V_{\text{refl}} + K_p K_2 \Delta V_2 V_{\text{refl}} \\ & - K_p K_2 K_{w2} \Delta V_2 V_{\text{refl}} \\ & - K_p K_2 K_{w2} \Delta V_2^2 - K_p V_c V_{\text{refl}} \\ & - K_p V_c \Delta V_2 + K_p K_2 K_{w2} V_c \Delta V_2 \\ & - K_p K_2 V_c \Delta V_2 + 2K_p K_{w2} V_c \Delta V_2 \\ & - K_p K_{w2}^2 V_c \Delta V_2 + 2K_p K_{w2} V_c V_{\text{refl}} \\ & - K_p K_{w2}^2 V_c V_{\text{refl}} - K_1 K_{w2} \Delta V_2 V_{\text{refl}} - K_p K_1 V_c \Delta V_2. \end{aligned}$$

ACKNOWLEDGMENT

The authors would like to thank Dr. E. Santi, University of South Carolina, and colleagues in the UCI Power Electronics Laboratory for many valuable discussions.

REFERENCES

[1] Q. Chen, F. C. Lee, and M. M. Jovanovic, "Analysis and design of weighted voltage-mode control for a multiple-output forward converter," in *Proc. APEC'93, 8th Annu.p Appl. Power Electron. Conf. Expo.*, San Diego, CA, Mar. 7–11, 1993, pp. 449–455.

[2] T. G. Wilson Jr., "Cross regulation in an energy-storage dc to dc converter with two regulated outputs," in *Proc. IEEE Power Electron. Spec. Conf. 1977 Rec.*, 1977, pp. 190–199.

[3] J. Marrero, "Improving cross regulation of multiple output flyback converters," in *Proc. 31st Int. Power Conversion Electron.'95*, Long Beach, CA, Sept. 9–15, 1995, pp. 357–365.

[4] D. C. Hamill and T. P. C. Yeo, "Characterization of cross regulation in dc–dc converters," in *Proc. INTELEC'93, 15th Int. Telecommun. Energy Conf.*, New York, NY, 1993, pp. 372–378.

[5] M. Goldman and A. F. Witulski, "Predicting regulation for a multiple-output current-mode controlled dc-to-dc converter," in *Proc. APEC'93, 8th Annu. Appl. Power Electron. Conf. Expo. Conf.*, pp. 617–623.

[6] K. H. Liu, "Effects of leakage inductances on the cross regulation in discontinuous-mode flyback converter," in *Proc. 4th Int. Conf. High frequency Power Conversion*, May 1989, pp. 254–259.

[7] S. Birca-Galateanu and X. Ivascu, "Frequemcy domain analysis of double dc–dc converters and of the dc–dc converters with multiple outputs," in *Electrtechnique Et Energetique*. Rome, Italy: Editua Academiei Romane, 1990.

[8] D. Maksimovic, R. Erickson, and C. Griesbach, "Modeling of cross regulation in converters containing coupled inductors," in *Proc. IEEE Appl. Power Electron. Conf.*, 1998, pp. 350–356.

[9] I. D. Jitaru, "DC–DC converter technologies," in *Proc. Sem. PAC 23, Power Syst. World*, Las Vegas, NV, 1996.

Chuanwen Ji received the B.S. degree in electrical engineering from Huazhong University of Science and Technology, Wuhan, China, in 1987, and the M.S. degree from the Institute of Electrical Engineering (IEE), Chinese Academy of Science (CAS), Beijing, in 1990.

He was an Assistant Researcher Professor from 1990 to 1995 and an Associate Research Professor, in 1996 at the IEE CAS, where he did research, development, and design of dc to dc power conversions and digital servo motor drives to control permanent magnetic synchronous motors (PMSM). In 1997, he was a Visiting Scientist at the Control Engineering Department, Fraunhofer-Institute of Production Systems and Design Technology, Berlin, Germany, for eight months. From 1997 to 2000, he was a Visiting Researcher at UCI Power Electronics Laboratory, University of California, Irvine. Presently, he is a Senior Design Engineer with Anacon Systems, Inc, working on single phase induction motor drives and microprocessor digital control. His interests include power electronics, power converter analysis and design, PFC technique, magnetics design, motor drives and servo motion control, digital systems design, and real-time control firmware implementation.

K. Mark Smith, Jr. (M'93) received the B.S. degree in electrical and computer engineering from the University of Colorado, Boulder, in 1990, and the M.S. and Ph.D. degrees in electrical engineering from the University of California, Irvine, in 1995 and 1999, respectively.

Since 1999, he has been working in industry designing high power converters and amplifiers. He has published more than 12 conference and journal papers in the area of power electronics. His research interests include soft switching of power converters, and precision analog and digital control of switching power amplifiers. He has been awarded a U.S. patent in the area of power electronics.

Keyue M. Smedley (SM'97) received the B.S. and M.S. degrees in electrical engineering from Zhejiang University, Hangzhou, China, in 1982 and 1985, respectively, and the M.S. and Ph.D. degrees in electrical engineering from the California Institute of Technology, Pasadena, in 1987 and 1991, respectively.

She was an Engineer at the Superconducting Super Collider from 1990 to 1992, where she designed and specified ac–dc conversion systems for all accelerator rings. She joined the faculty of the Electrical and Computer Engineering Department, University of California, Irvine, in 1992, where she has established the state-of-the-art Power Electronics Laboratory. Her research interest includes control, topologies, and integration of dc–dc converters, high fidelity class-D power amplifiers, active and passive soft switching techniques, single-phase and three-phase power factor correction and active power filter methods, and grid-connected inverters for alternative energy sources, etc.

Dr. Smedley is a member of Eta Kappa Nu and the Power Sources Manufacturer's Association. She is an Art-Large AdCom member of the IEEE Power Electronics Society, the Chair of IEEE Power Electronics Society Constitution and Bylaws Committee, and an Associate Editor of the IEEE TRANSACTIONS ON POWER ELECTRONICS.

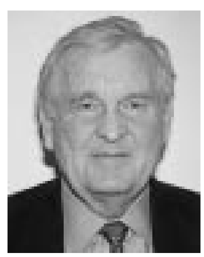

Ken King (M'00) received the B.S.E.E. and M.S.E.E. degrees from the University of Wisconsin, Madison, in 1951 and 1952, respectively.

From 1953 through 1971, he held technical-management positions at the Aberdeen Proving Ground, Aberdeen, MD, and National Cash Register, Mesa Scientific and Planning Research Corporation in Southern California, dominantly in areas of digital and analog circuit development associated with computers and control systems. He holds a number of patents related to those developments. Since 1972, he has been associated with technology based companies as an entrepreneur, in both founding and executive management capacities. He was President of Data Industries, Inc., from 1972 to 1975, a disk-drive-head manufacturing company, President of Delphi Communications Corporation, from 1972 to 1982, a developer of a multimedia communication center, and Executive Vice President of Cherokee International, LLC, from 1982 to 2000, a manufacturer of SMPS for computer and communications applications. Throughout these activities he was an active participant in the technical developments undertaken by these companies.